



Self-Propelled Janus Particles in a Ratchet: Numerical Simulations

Pulak K. Ghosh,¹ Vyacheslav R. Misko,^{1,2} Fabio Marchesoni,^{1,3} and Franco Nori^{1,4}

¹*CEMS, RIKEN, Saitama, 351-0198, Japan*

²*Department Fysica, Universiteit Antwerpen, B-2020 Antwerpen, Belgium*

³*Dipartimento di Fisica, Università di Camerino, I-62032 Camerino, Italy*

⁴*Physics Department, University of Michigan, Ann Arbor, Michigan 48109-1040, USA*

(Received 6 May 2013; published 24 June 2013)

Brownian transport of self-propelled overdamped microswimmers (like Janus particles) in a two-dimensional periodically compartmentalized channel is numerically investigated for different compartment geometries, boundary collisional dynamics, and particle rotational diffusion. The resulting time-correlated active Brownian motion is subject to rectification in the presence of spatial asymmetry. We prove that ratcheting of Janus particles can be orders of magnitude stronger than for ordinary thermal potential ratchets and thus experimentally accessible. In particular, autonomous pumping of a large mixture of passive particles can be induced by just adding a small fraction of Janus particles.

DOI: [10.1103/PhysRevLett.110.268301](https://doi.org/10.1103/PhysRevLett.110.268301)

PACS numbers: 82.70.Dd, 36.40.Wa, 87.15.hj

Rectification of Brownian motion has been the focus of a concerted effort, both conceptual [1] and technological [2], aimed at establishing net particle transport on a periodic substrate in the absence of external biases. To this purpose two basic ingredients are required (Pierre Curie's conjecture): a spatial asymmetry of the substrate and a time correlation of the (nonequilibrium) fluctuations, random or deterministic, applied to the diffusing particles. Each particle is assumed to interact with the substrate via an appropriate periodic potential, also called ratchet potential. Typically, demonstrations of the ratchet effect had recourse to external unbiased time-dependent drives (rocked and pulsated ratchets); rectification induced by time-correlated, or colored, fluctuations (thermal ratchets) seems to be of no practical use, despite its conceptual interest.

Brownian diffusion in a narrow, corrugated channel can also be rectified according to Curie's conjecture. The constituents of a mixture of repelling particles in a periodically modulated channel, are pressed against the channel walls so that their dynamics becomes sensitive to any asymmetry of the channel compartments (collective geometric ratchet). Subjected to an *ac* drive oriented along the channel axis, the mixture drifts in the easy-flow direction, where the average compartment corrugation is the less steep [3], although with much lower efficiency than in ordinary ratchet potentials. Such a collective ratchet mechanism has been experimentally observed for *ac* drives and relatively high particle densities [4,5], whereas the net current apparently vanishes at low densities [3]. A simple kinetic equation argument [6,7] suggests that rectification of mixtures of repelling particles, or even single particles, in an asymmetric channel can also be induced by time-correlated thermal fluctuations, like in thermal ratchets. However, being thermal ratchets weak in general and (low-density) collective geometric ratchets less performing than potential ratchets, demonstration of such an effect

seems beyond reach. On the other hand, rectification of Brownian diffusion by an internal energy source, like the nonequilibrium fluctuations invoked to power thermal ratchets, is very appealing: The diffusing particles would harvest kinetic energy directly from their environment, without requiring any externally applied field (though unbiased), and transport would ensue as an autonomous symmetry-directed particle flow.

To enhance rectification of time correlated diffusion in a modulated channel with zero drives, we propose to use a special type of diffusive tracers, namely of active, or self-propelled, Brownian particles. Self-propulsion is the ability of most living organisms to move, in the absence of external drives, thanks to an "engine" of their own [8]. Self-propulsion of micro- and nanoparticles (artificial microswimmers) poses a challenge with respect to their unusual nonequilibrium diffusion properties as well as their applications to nanotechnology [9]. Recently, a new type of microswimmers has been synthesized, where self-propulsion takes advantage of the local gradients that asymmetric particles can generate in the presence of an external energy source (self-phoretic effect). Such particles, called Janus particles [10], consist of two distinct "faces," only one of which is chemically or physically active. Such two-faced objects can induce either concentration gradients, by catalyzing some chemical reaction on their active surface [11,12], or thermal gradients, by inhomogeneous light absorption (self-thermophoresis) [13,14] or magnetic excitation (magnetically induced self-thermophoresis [15]). Moreover, experiments demonstrated the ability of Janus microswimmers to perform guided motions through periodic arrays [14] and separate colloidal mixtures, due to their selective interaction with the constituents of the mixture [16].

An active microswimmer gets a continuous push from the environment, which in the overdamped regime (inertia

effects are generally neglected) corresponds to a self-propulsion velocity \mathbf{v}_0 with constant modulus v_0 and direction randomly varying in time with rate τ_θ^{-1} . In a two-dimensional (2D) boundless suspension, the position $\mathbf{r}(t) = (x(t), y(t))$ of the microswimmer diffuses according to F urth's law

$$\langle \Delta \mathbf{r}(t)^2 \rangle = 4(D_0 + v_0^2 \tau_\theta / 4)t + (v_0^2 \tau_\theta^2 / 2)(e^{-2t/\tau_\theta} - 1), \quad (1)$$

where $\Delta \mathbf{r}(t) = \mathbf{r}(t) - \mathbf{r}(0)$ and D_0 is the translational diffusion constant of a passive particle of the same geometry at a fixed temperature. The mechanisms responsible for translational and rotational diffusion are not necessarily the same [12, 17] and therefore D_0 , v_0 , and τ_θ can be treated as independent model parameters. The diffusion law of Eq. (1) is due to the combined action of two statistically independent 2D Gaussian noise sources [18], a delta-correlated thermal noise, $\xi_\theta(t)$ and a colored effective propulsion noise, $\xi_c(t)$, with correlation functions $\langle \xi_{0,i}(t) \rangle = 0$, $\langle \xi_{c,i}(t) \rangle = 0$, $\langle \xi_{0,i}(t) \xi_{0,j}(0) \rangle = 2D_0 \delta_{ij} \delta(t)$, and $\langle \xi_{c,i}(t) \xi_{c,j}(0) \rangle = 2(D_c / \tau_\theta) \delta_{ij} e^{-2|t|/\tau_\theta}$, with $i, j = x, y$ and $D_c = v_0^2 \tau_\theta / 4$. Correspondingly, the microswimmer mean self-propulsion path is $l_\theta = v_0 \tau_\theta$.

When confined to a constrained geometry, like a channel, with compartment size smaller than the self-propulsion length, l_θ , the microswimmer undergoes multiple collisions with the walls and the confining geometry comes into play (Knudsen diffusion [19]). Contrary to standard thermal ratchets in asymmetric potentials [20], where the strength of the colored noise is kept constant, here D_c grows linearly with τ_θ [i.e., the variance of $\xi_c(t)$ is set to v_0^2]. As a consequence, increasing τ_θ not only makes geometric rectification effective even in the case of a single particle, but also enhances the power dissipated to fuel its self-propulsion. As a result, rectification in active Brownian ratchets can be so much stronger than in ordinary thermal ratchets that *direct observation* becomes possible. For instance, our simulations show that even a small fraction of interacting microswimmers suffices to drag along a large mixture of passive particles (autonomous pumping).

Autonomous Janus ratchets.—The rectification of a Janus particle in a 2D asymmetric channel was simulated by numerically integrating the Langevin equations [18], $\dot{x} = v_0 \cos \theta + \xi_{0,x}(t)$, $\dot{y} = v_0 \sin \theta + \xi_{0,y}(t)$, $\dot{\theta} = \xi_\theta(t)$, where $\xi_{0,x}(t)$ and $\xi_{0,y}(t)$ have been defined above and $\xi_\theta(t)$ is an additional 1D Gaussian noise with $\langle \xi_\theta(t) \rangle = 0$ and $\langle \xi_\theta(t) \xi_\theta(0) \rangle = 2D_\theta \delta(t)$, modeling the fluctuations of the self-propulsion angle θ , measured, say, with respect to the *positive* channel easy-flow direction. As $\langle \cos \theta(t) \cos \theta(0) \rangle = \langle \sin \theta(t) \sin \theta(0) \rangle = (1/2)e^{-|t|/D_\theta}$, it follows immediately that, in the notation of Eq. (1), $v_0 \cos \theta$ and $v_0 \sin \theta$ play the role of $\xi_{c,x}(t)$ and $\xi_{c,y}(t)$, respectively, with $\tau_\theta = 2/D_\theta$. The channel compartments were taken triangular in shape, with length x_L , width y_L and pore size Δ [see inset in Fig. 1(a)]. Throughout our

simulations we kept the compartment aspect ratio $r = x_L/y_L$ constant with $r = 1$, and, by rescaling $x \rightarrow x/\kappa$ and $y \rightarrow y/\kappa$, we conveniently set $x_L = y_L = 1$. Analogously, we rescaled $t \rightarrow v_0 t/\kappa$, so as to work with a constant self-propulsion velocity, $v_0 = 1$. In summary, the output of our integration code only depends on two rescaled noise intensities, $D_0/\kappa v_0$ and $\kappa D_\theta/v_0$ (or, equivalently, $v_0 \tau_\theta/\kappa$), and one geometric parameter Δ/y_L .

The collisional dynamics of a Janus particle at the boundaries was modeled as follows. The translational velocity $\dot{\mathbf{r}}$ is elastically reflected, whereas for the coordinate θ we considered two possibilities. (i) Frictionless collisions, θ unchanged. The microswimmer slides along the walls for an average time of the order of τ_θ , until the noise $\xi_\theta(t)$ redirects it toward the center of the compartment. The inset in Fig. 1(a) clearly shows the accumulation of the stationary particle probability density $P(x, y)$ along the boundaries. (ii) Rotation induced by a tangential friction, θ randomized. This causes the particle to diffuse away from the boundary, which in general weakens the

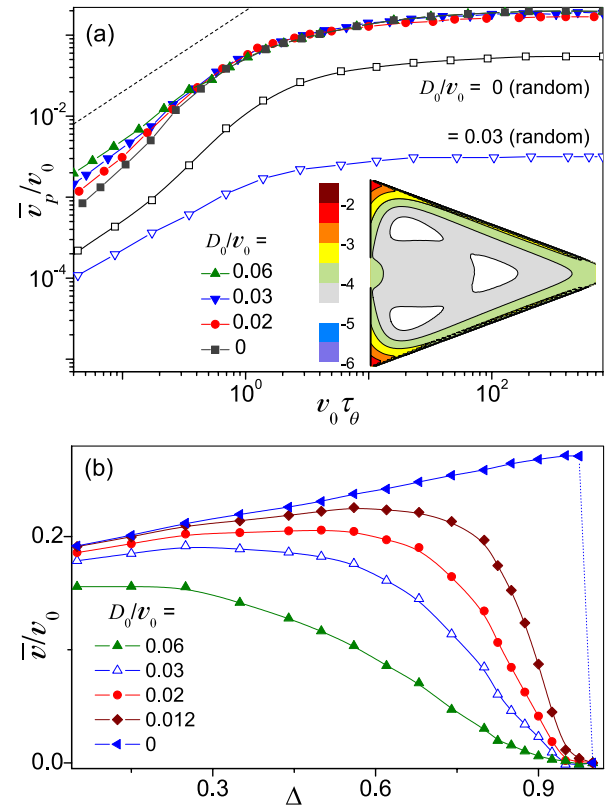


FIG. 1 (color online). Rectification of a single pointlike Janus particle with self-propulsion speed v_0 in a triangular channel with compartment size $x_L = y_L = 1$: (a) average velocity \bar{v} vs τ_θ for channel pore size $\Delta = 0.1$, different D_0 and sliding (closed symbols), or randomized *bc* (open symbols). A dashed line with slope 1 is drawn for the reader's convenience. Inset: (logarithmic) contour plot of the stationary probability density $P(x, y)$ in a channel compartment; (b) average \bar{v} vs Δ for different D_0 , sliding *bc*, and $\tau_\theta = 300$.

rectification effect [see Fig. 1(a)]. Note that in the case of elastic boundary reflection of both $\dot{\mathbf{r}}$ and \mathbf{v}_0 , the microswimmer motion would amount to an ordinary equilibrium Brownian diffusion with finite damping constant, $\gamma = 2/\tau_\theta$ [21], and rectification would be suppressed.

In Fig. 1 we report our results for the rectification current, $\bar{v} \equiv \langle \dot{x} \rangle$ (in units of v_0), of a pointlike Janus particle in a triangular channel with fixed compartment dimensions and varying τ_θ , panel (a), and Δ , panel (b). In panel (a) the pore size was set to $\Delta = 0.1$ and several curves \bar{v} versus τ_θ were computed for different D_0 , i.e., at different temperatures, and sliding boundary conditions (*bc*, filled symbols). At large τ_θ , microswimmer diffusion is of the Knudsen type and rectification is dominated by self-propulsion; all curves $\bar{v}(\tau_\theta)$ increase monotonically with τ_θ until they level off [the weak D_0 dependence of such asymptotes is shown in Fig. 1(b)]. Most importantly, we obtained ratios \bar{v}/v_0 in excess of 20%, which means that here the rectification power is orders of magnitude larger than for single-particle thermal ratchets in an asymmetric potential [2]. Moreover, the simulation parameter values adopted here, in rescaled units, are consistent with the corresponding values reported in the experimental literature, see, e.g., Table 1 of Ref. [14], hence, the possibility of a direct demonstration of this striking effect.

For the sake of a comparison in panel (a) we also report two curves $\bar{v}(\tau_\theta)$ obtained by imposing θ randomization at the boundaries (empty symbols). As expected \bar{v}/v_0 decreases as the persistency of the particle self-propulsion is suppressed by its collisions against the walls. The thermal fluctuations $\xi_0(t)$ further suppress rectification as they induce more wall collisions and, thus, stronger θ randomization at the boundaries. In other words, randomized *b.c.* tend to statistically couple thermal fluctuations and random self-propulsion mechanism. Finally, we notice that the curves $\bar{v}(\tau_\theta)$ at low τ_θ shift upwards on raising the thermal noise level D_0 . This effect becomes apparent for $l_\theta < x_L$, that is, for τ_θ smaller than the average time a self-propelled particle takes to exit a compartment. Under such circumstances, thermal noise assists the rectification process. Moreover, on taking the long-time limit of the diffusion law in Eq. (1), $\langle \Delta \mathbf{r}(t)^2 \rangle = 4(D_0 + D_c)t$, we see that at even smaller self-propulsion lengths, $l_\theta < 4D_0/v_0$, self-propulsion can be neglected with respect to thermal fluctuations.

Panel (b) of Fig. 1 illustrates the dependence of \bar{v} on the pore size for increasing D_0 at large τ_θ and sliding *bc*. Here the rectification power is suppressed by the thermal fluctuations and is the highest for large Δ . The first trend is opposite to that observed for low τ_θ : now $\xi_0(t)$ helps the Janus particle bypass the compartment corners, when \mathbf{v}_0 pushes it in the negative direction [see inset of panel (a)]. Therefore, the diode-funneling effect exerted by the triangular compartments can be either enhanced or weakened by delta-correlated fluctuations, depending on the regime

of self-propulsion. The second trend might sound counter-intuitive, were not that for larger Δ and fixed y_L the sides of the channel grow shorter and the particle takes less time to slide along them and through the exit pore. On the other hand, the backward flow with negative velocity is blocked mostly at the compartment corners, regardless of the actual pore size. The moderate Δ dependence reported in Fig. 1(b) indicates that our numerical analysis can be safely extended to Janus swimmers of finite radius.

Finally, in view of practical applications, we tested the robustness of Janus particle rectification in channels with variable degrees of asymmetry. In Fig. 2 we varied the channel geometry by symmetrically shifting the compartment corners by a fixed amount $x_0 \in [0, 0.5)$ (see inset). Moreover, we also enlarged the compartments by a scaling factor κ , so as to accommodate for a variety of experimental set-ups. One immediately sees that the rectification power decreases by only a factor 2 for x_0 up to 0.2 and is insensitive to κ as long as $l_\theta > \kappa x_L$. For much larger κ , the particle spends most of its time away from the (asymmetric) compartment walls and \bar{v} drops inversely proportional to κ . Indeed, the rescaled intensity of $\xi_0(t)$, $D_0/\kappa v_0$, is suppressed with respect to the rescaled propulsion noise intensity, $D_c = \kappa D_\theta/v_0$, which means that for $\kappa \rightarrow \infty$, $\kappa \bar{v}/v_0$ tends to a constant, that is, $\bar{v} \propto \kappa^{-1}$ [see curves for $D_0 = 0$ in Fig. 1(a)].

Janus particles as autonomous pumps.—The remarkable robustness of the rectification mechanism investigated here lends itself to practical applications. Let us consider a binary mixture consisting of N_m Janus microswimmers with large l_θ (active particles) and N_p non-self-propelling objects (passive particles). For simplicity, both species are represented by soft interacting disks of radius r_0 and repulsive force of modulus $F_{i,j} = k(2r_0 - r_{ij})$ if $r_{ij} < 2r_0$

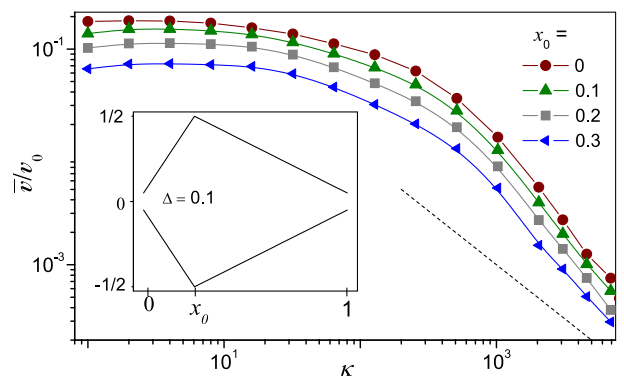


FIG. 2 (color online). Rectification of single Janus particle with $v_0 = 1$ in asymmetric channels with different geometries. A typical compartment is sketched in the inset: x_L , y_L , and Δ are as in Fig. 1(a), i.e., $\kappa = 1$, but the corners are shifted by x_0 . The compartment dimensions have then be rescaled by a magnification factor κ . Main panel: average velocity \bar{v} versus κ for $\tau_\theta = 300$, sliding *bc* and different x_0 . A dashed line with slope -1 is drawn for the reader's convenience.

and $F_{i,j} = 0$ otherwise (F_{ij} and r_{ij} denote, respectively, the pair force and distance) [18]. Other potentials have also been tested with qualitatively similar results, namely, (i) active microswimmers are capable of rectifying their motion even through a crowd of passive particles, i.e., for packing fractions $\phi = 2\pi r_0^2 N_t / x_L y_L$ in excess of 1 (particles of either species overlap in average by a length $l_0 = v_0/k$ and can even pass each other); and, (ii) due to their finite size and repulsive interaction with all mixture constituents, even a low fraction of Janus microswimmers suffices to set the entire mixture in motion (autonomous pumping).

Autonomous pumping of a binary mixture of $N_t = N_m + N_p$ soft disks was simulated under simplifying assumptions: (i) In the bulk, the microswimmer orientation randomly changes at time intervals τ_θ with θ uniformly distributed in $[0, 2\pi)$, which is equivalent to setting $D_\theta = \pi^2/6\tau_\theta$; (ii) collisions with the walls only take place when the center of the disks hit the boundary, disks are not elastically repelled by the walls [see inset of Fig. 3(c)]; (iii) zero thermal fluctuations, $D_0 = 0$, randomized bc (i.e., θ diffusion is stronger close to the walls than in the bulk) were assumed for the active microswimmer dynamics in order to demonstrate the pumping effect under the least favorable conditions. Under sliding bc pumping is appreciably stronger (not shown).

Our simulation results are reported in Fig. 3. A few general properties, largely independent of the model details, are discussed here. First, the mixture drifts in the easy-flow (positive) direction, the average velocities of the active and passive particles being, respectively, \bar{v}_m and \bar{v}_p . In particular, the rectification power, \bar{v}_p/v_0 , is no smaller than reported for potential ratchets [2]. Second, for any given choice of the model parameters, there exists an optimal N_t where the pumping is the strongest. This defines an optimal pumping active fraction, typically with $N_m/N_t < 0.1$. Third, pumping is clearly fueled by active microswimmers as proven by \bar{v}_p dropping for $l_0 \lesssim x_L$ [panel (a)] and surging with increasing the interaction constant, k [panel (d)], or the fraction of active particles (not shown). For harder disks, optimal pumping occurs at larger τ_θ because a Janus disk takes more time (and a longer random path) to cross a compartment crowded with more strongly repelling disks. As for the case of Fig. 1(b), the pore size Δ is clearly less important as a control parameter than τ_θ and k [panel (d)]. Finally, we notice that for dense mixtures, $\phi \sim 1$, the microswimmer velocity \bar{v}_m can reverse sign. This effect was anticipated for binary mixtures on a ratchet [22]: passive particles accumulate preferably on the right-hand side of the pore, where the cross section is the largest; passive particle thus act upon the diluted Janus microswimmers as an asymmetric repulsive potential barrier, which can supersede the funneling action of the compartment walls, hence, the Janus current inversion at high N_t .

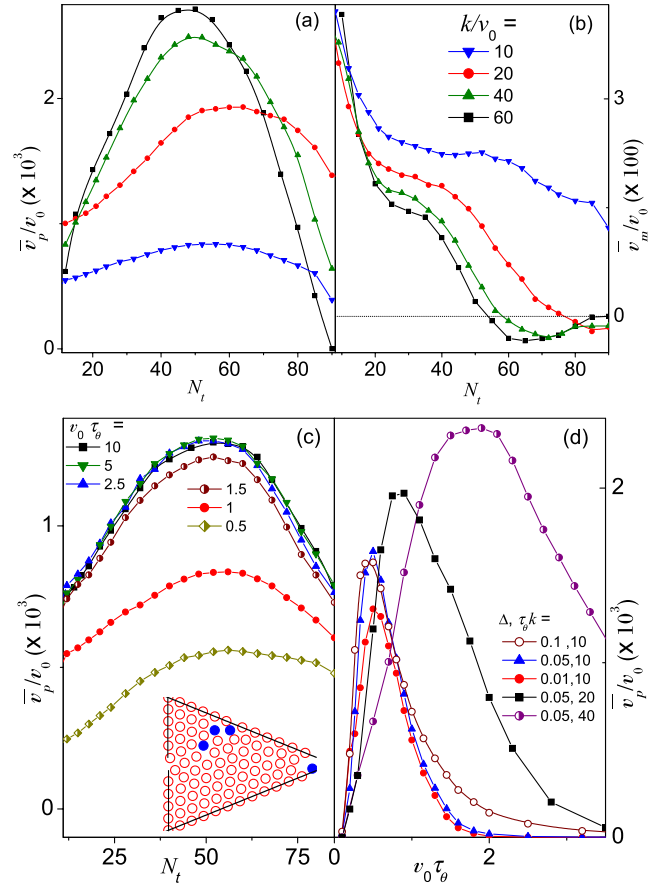


FIG. 3 (color online). Rectification of a binary mixture made of $N_m = 4$ Janus particles with self-propulsion speed v_0 , $D_0 = 0$, and $N_p = N_t - N_m$ passive particles. All particles are modeled as elastically repelling soft disks of radius $r_0 = 0.05$; channel compartments are triangular with dimensions $x_L = y_L = 1$. In the inset, active and passive particles are represented by (blue) closed and (red) open circles, respectively. Panels (a) and (b) show average rectification velocity (a) of passive, \bar{v}_p and (b) active particles, \bar{v}_m , versus N_t for $\Delta = 0.1$ and different interaction constant, k [see legend in (b)]. (c) \bar{v}_p vs N_t for $\Delta = 0.1$ and different τ_θ ; (d) \bar{v}_p vs τ_θ for $N_t = 72$ and different Δ and k . Note that $l_0 = v_0/k$ is a measure of the disk overlap, so that $\tau_\theta k = l/l_0$.

To conclude, we stress that the autonomous rectification and pumping effects discussed here apply to biological and artificial swimmers regardless of their propulsion mechanism, and not only to especially fabricated Janus particles. For instance, the autonomous robots of Ref. [23] are laser driven with propulsion speed v_0 and about $10 \mu\text{m}$ across, which means that their translational diffusion is negligible. The diffusion of their propulsion orientation is due to the scattering by spatial disorder, that is, $\tau_\theta \sim l/v_0$, where l is a disorder correlation length. In cellular systems, propulsion of macromolecules can be fueled by the “power-stroke” associated with the hydrolysis of ATP in suspension. In that case, $v_0 \sim \delta r/\tau_\theta$, where δr is the net displacement produced by a single power-stroke and τ_θ^{-1}

coincides with the ATP hydrolyzation rate in the vicinity of the biomolecule [19].

We thank RICC for computational resources. P. K. G. acknowledges financial support from JSPS through fellowship No. P11502. V. R. M. acknowledges support from the Odysseus Program of the Flemish Government and FWO-VI. F. M. acknowledges partial support from the European Commission, Grant No. 256959 (NanoPower). F. N. was supported in part by the ARO, RIKEN iTHES Project, JSPS-RFBR Contract No. 12-02-92100, Grant-in-Aid for Scientific Research (S), MEXT Kakenhi on Quantum Cybernetics, and the JSPS via its FIRST program.

-
- [1] P. Reimann, *Phys. Rep.* **361**, 57 (2002).
- [2] P. Hänggi and F. Marchesoni, *Rev. Mod. Phys.* **81**, 387 (2009); P. Hänggi, F. Marchesoni, and F. Nori, *Ann. Phys. (Berlin)* **14**, 51 (2005).
- [3] J. F. Wambaugh, C. Reichhardt, C. J. Olson, F. Marchesoni, and F. Nori, *Phys. Rev. Lett.* **83**, 5106 (1999).
- [4] J. E. Villegas, S. Savel'ev, F. Nori, E. M. Gonzalez, J. V. Anguita, R. García, and J. L. Vicent, *Science* **302**, 1188 (2003); Y. Togawa, K. Harada, T. Akashi, H. Kasai, T. Matsuda, F. Nori, A. Maeda, and A. Tonomura, *Phys. Rev. Lett.* **95**, 087002 (2005); C. C. de Souza Silva, J. Van de Vondel, M. Morelle, and V. V. Moshchalkov, *Nature (London)* **440**, 651 (2006); N. S. Lin, T. W. Heitmann, K. Yu, B. L. T. Plourde, and V. R. Misko, *Phys. Rev. B* **84**, 144511 (2011).
- [5] D. Cole, S. Bending, S. Savel'ev, A. Grigorenko, T. Tamegai, and F. Nori, *Nat. Mater.* **5**, 305 (2006).
- [6] R. Zwanzig, *J. Phys. Chem.* **96**, 3926 (1992).
- [7] for a review see P. S. Burada, P. Hänggi, F. Marchesoni, G. Schmid, and P. Talkner, *ChemPhysChem* **10**, 45 (2009).
- [8] E. M. Purcell, *Am. J. Phys.* **45**, 3 (1977).
- [9] F. Schweitzer, *Brownian Agents and Active Particles* (Springer, Berlin, 2003); P. Romanczuk, M. Bär, W. Ebeling, B. Lindner, and L. Schimansky-Geier, *Eur. Phys. J. Special Topics* **202**, 1 (2012).
- [10] *Janus Particle Synthesis, Self-Assembly and Applications*, edited by S. Jiang and S. Granick (RSC Publishing, Cambridge, 2012); A. Walther and A. H. E. Müller, *Chem. Rev.* (2013).
- [11] W. F. Paxton, S. Sundararajan, T. E. Mallouk, and A. Sen, *Angew. Chem., Int. Ed.* **45**, 5420 (2006).
- [12] J. G. Gibbs and Y.-P. Zhao, *Appl. Phys. Lett.* **94**, 163104 (2009); J. R. Howse, R. A. L. Jones, A. J. Ryan, T. Gough, R. Vafabakhsh, and R. Golestanian, *Phys. Rev. Lett.* **99**, 048102 (2007).
- [13] H. R. Jiang, N. Yoshinaga, and M. Sano, *Phys. Rev. Lett.* **105**, 268302 (2010).
- [14] G. Volpe, I. Buttinoni, D. Vogt, H.-J. Kümmerer, and C. Bechinger, *Soft Matter* **7**, 8810 (2011).
- [15] L. Baraban, R. Streubel, D. Makarov, L. Han, D. Karnausenko, O. G. Schmidt, and G. Cuniberti, *ACS Nano* **7**, 1360 (2013).
- [16] W. Yang, V. R. Misko, K. Nelissen, M. Kong, and F. M. Peeters, *Soft Matter* **8**, 5175 (2012).
- [17] S. van Teeffelen and H. Löwen, *Phys. Rev. E* **78**, 020101 (R) (2008).
- [18] Y. Fily and M. C. Marchetti, *Phys. Rev. Lett.* **108**, 235702 (2012).
- [19] H. Brenner and D. A. Edwards, *Macrotransport Processes* (Butterworth-Heinemann, New York, 1993).
- [20] R. Bartussek, P. Reimann, and P. Hänggi, *Phys. Rev. Lett.* **76**, 1166 (1996).
- [21] P. K. Ghosh, P. Hänggi, F. Marchesoni, F. Nori, and G. Schmid, *Europhys. Lett.* **98**, 50002 (2012); *Phys. Rev. E* **86**, 021112 (2012).
- [22] S. Savel'ev, F. Marchesoni, and F. Nori, *Phys. Rev. Lett.* **91**, 010601 (2003); **92**, 160602 (2004).
- [23] A. Búzás, L. Kelemen, A. Mathesz, L. Oroszi, G. Vizsniczai, T. Vicsek, and P. Ormos, *Appl. Phys. Lett.* **101**, 041111 (2012).